

Chemical Evaluation and Quantum Analysis of Methanol Extracts of *Costus lucanusianus* as Corrosion Inhibitors for Mild Steel and Aluminium in 1 M HCl Solution.

Obot, A. S.^{1*}, Boekom, E. J.¹, Obot, I. B.², Ita, B. N.¹ and Azubuike, A. C.¹

¹Department of Chemistry, University of Uyo, P.M.B 1017, Uyo, Akwa Ibom State, Nigeria.

²Centre of Research Excellence in Corrosion, Research Institute, King Fahd University of Petroleum and Minerals, Dhahran, 31261, Saudi Arabia.

ARTICLE INFO

Article history:

Received: 11 March 2021;

Received in revised form:

6 October 2021;

Accepted: 18 October 2021;

Keywords

Corrosion,
Costus lucanusianus,
Quantum Chemical
Calculations,
Thermo-Gravimetric,
Thermodynamics.

ABSTRACT

Corrosion inhibition of mild steel in 1 M HCl solutions by methanol extracts of *Costus lucanusianus* was investigated at concentrations of 0.1 g/L, 0.2 g/L, 0.5 g/L, 0.7 g/L and 1 g/L using thermo-gravimetric analysis from 303 K – 333 K. Maximum inhibition efficiency of 88% and 86% for mild steel and aluminium was observed. The adsorption was found to obey Freundlich isotherm. GC-MS analysis showed major components of Methanol Stem Extract (MSE) and Methanol leave Extract (MLE) as 1,3-bis (3-bromophenyl) 1,3-propanedione (12.60%) and 3-hydroxyl-4-methoxy benzylalcohol (72.17%) respectively. Quantum chemical calculations using Density Functional Theory employing the Becke exchange functional and the Lee Yang Parr correlation functional (BLYP), together with the generalized gradient approximation (GGA) employing the “double numeric polarization” (DNP) basis sets was used in optimization of the geometries of the molecules. The inhibitors showed significant inhibitive effect following the trend MSE > MLE.

© 2021 Elixir All rights reserved.

1.0 Introduction

Mild steel has relatively low tensile strength although the surface hardness can be increased through carburizing. Mild steel is quite easy to cold-form, making it easier to handle and widely used in different fields of industries, automobiles, engineering and submarines due to its low cost. Typical application of mild steel are car parts, pipes, construction and food cans. However, proneness to corrosion is its greatest challenge. Its mechanical and cheap cost possibly accounts for its foremost use in several construction works; but its degradation when in contact with corrosion agents like acids, is a considerable issue for its extensive use (Sasikumar *et al.*, 2015).

Aluminium is almost always alloyed which markedly improves its mechanical properties. The major uses of aluminium are in transportation, packaging, electrical-related issues, machinery and equipment and a range of household items. Aluminium is an active metal and is naturally passivated forming an aluminium oxide film (Al_2O_3) on the metal surface. The oxide film can protect aluminium from corrosion in natural and some acid environments; however, it is expected to dissolve in alkalizes (Segneau *et al.*, 2012).

Acid medium is the most commonly used type of aggressive solution for pickling, cleaning, descaling and oil well acidification. Common inorganic pickling solutions include HCl, H_2SO_4 , and HNO_3 (Hsissou *et al.*, 2020). In the pickling process, HCl is superior to other acids because of the fact that HCl reduces pickling time and achieves better surface quality (Tan *et al.*, 2020). When using hydrochloric acid pickling solution to pickle metal surface, it will

inevitably cause different degrees of corrosion to the metal substrate. Therefore, the most commonly used methods is to diminution the harmful impacts of acid-induced corrosion by adding a small amount of corrosion inhibitor (Tan *et al.*, 2020). The addition of inhibitor to the pickling solution has become one of the significant methods for metal corrosion protection which is attributed to its simple operation, low cost, mature technology and remarkable protective effect (Olasunkanmi and Ebenso, 2020).

Corrosion has been a major threat to the operation of industries ranging from the questionable structural integrity of manufactured materials and equipment to the economic implications of corroded materials and safety. Numerous failures and eventual losses of equipment in the chemical industry have been traced to corrosion processes (Aralu *et al.*, 2021). There are reported cases where small amounts of moisture have caused corrosion in tablets with printed circuits, nichrome resistors, fittings, electrical connectors and a wide range of components, and micro-electronic components, which have been coated with metallic films (Valdez, *et al.*, 2006); (Lopez, *et al.*, 2007).

There has been increasing awareness of the environment and green chemistry (Uwah *et al.*, 2013a). Therefore, the research of green corrosion inhibitors which is environment friendly, has become a popular direction for many corrosion researchers thereby replacing harmful synthetic chemicals (Othman, *et al.*, 2019). Green corrosion inhibitors are biodegradable and do not contain heavy metals or other toxic compounds (Ituen and Udo, 2012). Natural corrosion inhibitors are extracted from herbs, medicinal plants, fruits,

vegetable peels and spices (Lakmal and Tillekaratne, 2018). Although, a number of plants and their phytochemicals have been reported as anticorrosive agents, vast majority of plants have not yet been properly studied for their anti-corrosive activity. For example, of the nearly 300,000 plant species that exist on the earth, only a few (less than 1%) of these plants have been completely studied relative to their anticorrosive activity (Uwah *et al.*, 2013b). Thus, enormous opportunities exist to find out novel, economical and eco-friendly corrosion inhibitors from this outstanding source of natural products (Saratha and Meenakshi, 2010). As such, *C. lucanusianus* stem and leave extracts are the main focus of this study which is aimed at investigating the its corrosion inhibition potential on mild steel and aluminium in 1 M HCl solution with insight into proposing the mechanism of its inhibitory action.

2.0 Materials And Methods

The mild steel (4×4 cm) and aluminium (3×3 cm) coupons obtained from Ken Johnson Nigeria Limited, an engineering outlet in Uyo, Akwa Ibom State, Nigeria. The elemental composition of the mild steel by weight percentage was carbon–0.17, silicon–0.26, manganese– 0.46, phosphorus – 0.0047, sulphur–0.017, iron – 98.935 and pure aluminium metal of the type AA 1060 were used in this investigation. The coupons were polished with series of emery paper of variable grades starting with the coarsest to the finest (1200) grade. Each coupon was degreased by washing with ethanol, dried with acetone and stored in a desiccator.

2.1 Preparation of *C. lucanusianus* extracts

Fresh *C. lucanusianus* stem and leaves were cut into small pieces and dried under room temperature. The dried samples were ground into powdered form, soaked in methanol for 72 hours and filtered. The filtrate was subjected to evaporation at 313 K to obtain samples free of methanol. The stock solutions of the *C. lucanusianus* extracts were used to prepared different concentrations of the extracts by dissolving 0.1 - 0.7 g of the extract in 1 L of 1 M HCl.

2.2 Identification of extract components

Gas Chromatography – Mass Spectrometry (GCMS) was used to separate the chemical mixtures and identify the components

2.3 Thermo-Gravimetric Analysis

The pre-cleaned coupons were weighed and suspended through a glass hook hanged on a rod into a test solution containing different concentrations of the extract. The system was maintained at 303 K. The weight loss with respect to time was determined by retrieving the coupons from the test solutions, washed in distilled water, scrubbed with bristled

brush, cleansed with ethanol, dried in acetone and reweighed at 2hours intervals progressively for 10hours. The experiment was repeated at 313 K, 323 K and 333 K. The weight loss was the difference between the initial and final weight of the coupons at 2hours intervals (Equation 1).

$$\Delta W = (W_0 - W_1) \text{ g} \quad (1)$$

From the experiment, the corrosion rate (CR), surface coverage (Θ) and inhibition efficiency (%IE) were computed using equations previously reported by Ituen and Udo (2012)

2.4 Quantum Chemical Calculations

Quantum chemical calculations using Density Functional Theory employing the Becke exchange functional and the Lee Yang Parr correlation functional (BLYP), together with the generalized gradient approximation (GGA) employing the “double numeric polarization” (DNP) basis sets was used in optimization of the geometries of the molecules. Electronic properties such as E_{HOMO} , E_{LUMO} and Energy gap were calculated and used to obtain the chemical reactivity parameters from DFT. These chemical reactivity parameters include: Ionization potential (IE), Electron affinity (EA), Energy gap (ΔE), Electronegativity (χ), Dipole moment (μ), Global hardness (η), Global softness (σ), Electrophilicity (ω), Nucleophilicity (ϵ), The fraction of electrons transported from *C. lucanusianus* to Fe surface (ΔN). These parameters were calculated using equations previously reported by Belghiti *et al.*, 2019; Ituen *et al.*, 2019; Saraswat *et al.*, 2020.

3.0 Results and Discussion

3.1 Gas Chromatography - Mass Spectrometry (GCMS) Analysis

Figure 1 shows the GC-MS chromatogram of the active chemical constituents of MSE and MLE

The retention time, compound, molecular formula, molecular mass and % peak area are presented in Table 1 and 2 for MSE and MLE. Among these twenty constituents, the GC-MS spectrum shows that it quantitatively contains most of 1,3-bis(3-bromophenyl)-1,3-propanedione for MSE, 3-hydroxy-4-methoxybenzylalcohol for MLE exhibiting the highest peak area of 12.60% and 72.17%, respectively. Therefore, these compounds are the predominant constituents. (Geetha and Udhayakumar, 2021; Mahgoub *et al.*, 2019).

3.2 Thermo-Gravimetric Measurements

The thermo-gravimetric graphs presented in Figures 2, 3, 4 and 5 show that weight loss (g) increased with time, decreased with increase in concentration of the inhibitor and increased with temperature. The decrease of weight loss with increase in concentration of the inhibitor can be attributed to the inhibitive effects of *C. lucanusianus*.

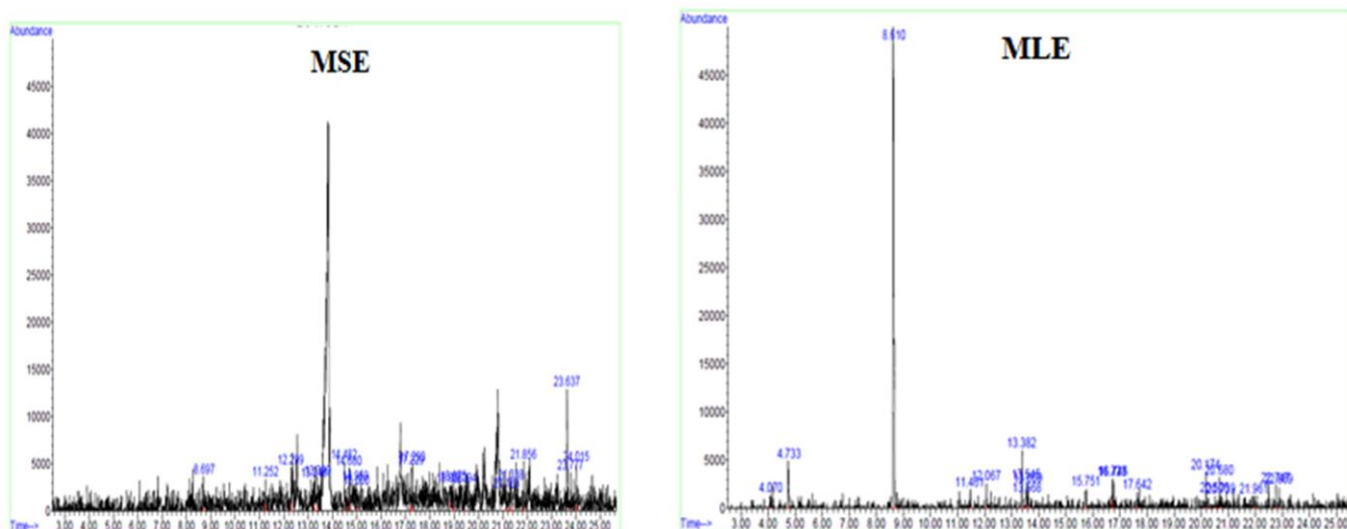


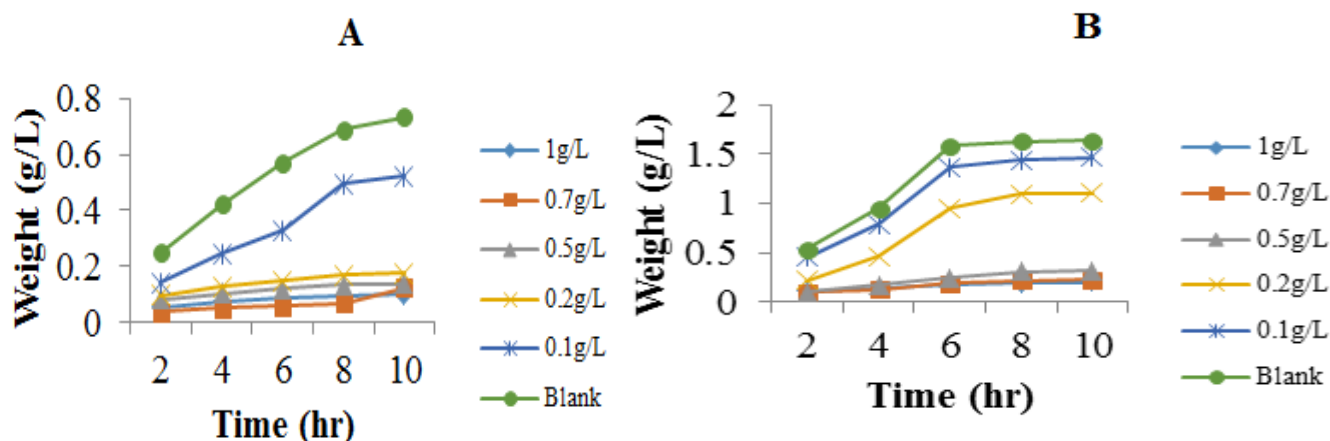
Figure 1. GCMS Chromatograms of MSE and MLE.

Table 1. MSE Components.

Peak no.	RT	Compound	Area (%)	Molecular formula	MM (g/mol)
1	8.697	4-Dimethylamino-3,5-dinitrobenzoic acid	3.65	C ₉ H ₉ N ₃ O ₆	255.18
2	11.252	4-(3-hydroxybutyl)-3,5,5-trimethyl-2-cyclohexen-1-one	4.35	C ₁₃ H ₂₂ O ₂	210.32
3	12.299	2-t-butylperoxy-2-ethylbutan-1-ol, butyrate ester	6.54	C ₁₄ H ₂₈ O ₄	260.37
4	13.248	1-methoxy-5-hexene	4.42	C ₇ H ₁₄ O	114.19
5	13.399	1,2,4,5-tetramethyl-3-pyrazolidinone	5.51	C ₇ H ₁₄ N ₂ O	142.20
6	14.482	2-(4,6-dimethyl-2-pyrimidinyl)-6-methyl-1H-pyrazolo[3,4b] pyridine 3,4-dione	7.21	C ₁₃ H ₁₃ N ₅ O ₂	271
7	14.680	Metanilic acid	3.66	C ₆ H ₇ NO ₃ S	173.19
8	14.959	3-methyl-1H-pyrazole	3.69	C ₄ H ₆ N ₂	82.19
9	15.000	Octadecanoic acid	3.77	C ₁₈ H ₃₆ O	284.50
10	17.229	1-cyclohexene-1-methanol	6.18	C ₇ H ₁₂ O	112.17
11	17.293	2-cyclobutene-1-carboxamide	4.04	C ₅ H ₇ NO	97.12
12	18.806	Trans-syn-tricyclo [7.3.0.0(2,6)]-8-dodecene	3.69	C ₁₂ H ₁₈	162.27
13	18.975	Tetrahydrothiazole	4.48	C ₃ H ₇ NO	89.16
14	19.394	4-[(3-aminophenyl) diphenyl methyl]-N,N-diethylbenzenamine	3.77	C ₃₃ H ₃₈ N ₂	462.70
15	21.163	2-propenal	3.65	C ₃ H ₄ O	56.06
16	21.338	1-acetyl-2,3-dihydro-6-nitro-1H-Indole	5.43	C ₁₀ H ₁₀ N ₂ O ₃	206.20
17	21.856	4-(p-Toluenesulfonamido) benzoic acid	4.02	C ₁₄ H ₁₃ NO ₄ S	291.32
18	23.637	1,3-bis(3-bromophenyl) 1,3-propanedione	12.60	C ₁₅ H ₁₀ Br ₂ O ₂	382.05
19	23.777	3-[4-[[4-chloro-6-(diethylamino)-1,3,5-triazin-2-yl]amino] phenyl] -2H-1-benzopyran-2-one	4.34	C ₂₂ H ₂₀ ClN ₅ O ₂	421.90
20	24.015	Stigmasta-4,6,22-trien-3.beta.-ol	4.99	C ₂₉ H ₄₆ O	410.70

Table 2. MLE Components.

Peak no.	RT	Compound	Area (%)	Molecular formula	MM (g/mol)
1	4.070	6,7 dimethoxy-3-phenyl 4H-1-benzopyran-4-one	0.70	C ₁₇ H ₁₄ O ₄	282.29
2	4.733	3-phenylquinoxaline -1- oxide	4.49	C ₁₄ H ₁₀ N ₂ O	222.24
3	8.610	3-hydroxy-4-methoxy benzyl alcohol	72.17	C ₈ H ₁₀ O ₃	154.16
4	11.461	N-cyano-2-methylazetidene	1.17	C ₅ H ₈ N ₂	96.13
5	12.067	1- methyl imidazole	1.34	C ₄ H ₆ N ₂	82.10
6	13.382	2-methyl furan	5.51	C ₅ H ₆ O	82.10
7	13.545	3-methoxy-1,3,4 hexatriene	0.99	C ₇ H ₁₀ O	110.15
8	13.568	Difluoramine	0.79	F ₂ HN	53.01
9	13.609	Methyl (4-nitrophenyl)carbamic acid	0.98	C ₈ H ₈ N ₂ O ₄	196.16
10	15.751	2-pentyn-1-ol	0.90	C ₅ H ₈ O	84.12
11	16.723	1,6 hexanediol	1.03	C ₆ H ₁₄ O ₂	118.17
12	16.746	3,4-dihydro-6-methyl-2H-pyran	1.31	C ₆ H ₁₀ O	98
13	17.642	4-carboxychloro-N-acetoxypiperidine	0.73	C ₈ H ₁₂ ClNO ₄	221
14	20.174	3-hydroxyiminocyclopentan-2-one-1-carboxylic acid	2.56	C ₆ H ₇ NO ₄	157.12
15	20.506	2-propenenitrile	0.73	C ₃ H ₃ N	53.06
16	20.680	2-propenenitrile	1.32	C ₃ H ₃ N	53.06
17	20.739	1-butene	0.70	C ₄ H ₈	56.11
18	21.961	2-propenenitrile	0.92	C ₃ H ₃ N	53.06
19	22.747	7-diethylamino-3-iodo-4-methyl-chromen-2-one	0.97	C ₁₄ H ₁₆ INO ₂	357.19
20	22.869	Tetrahydrothiazole	0.67	C ₃ H ₇ NS	89.16



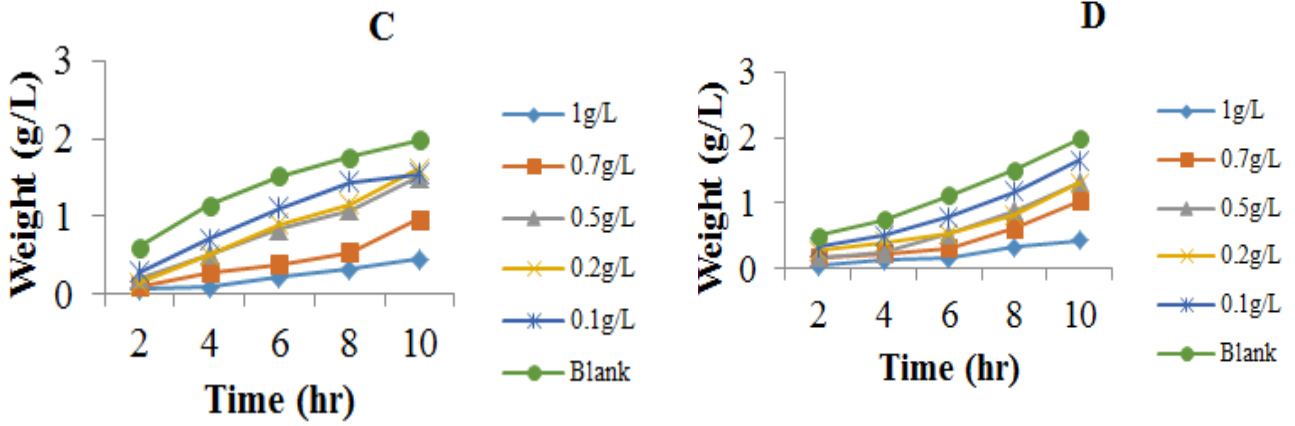


Figure 2. Variation of weight loss with time for the corrosion of mild steel in different concentrations of MSE at A (303 K), B (313 K), C (323 K) and D (333 K).

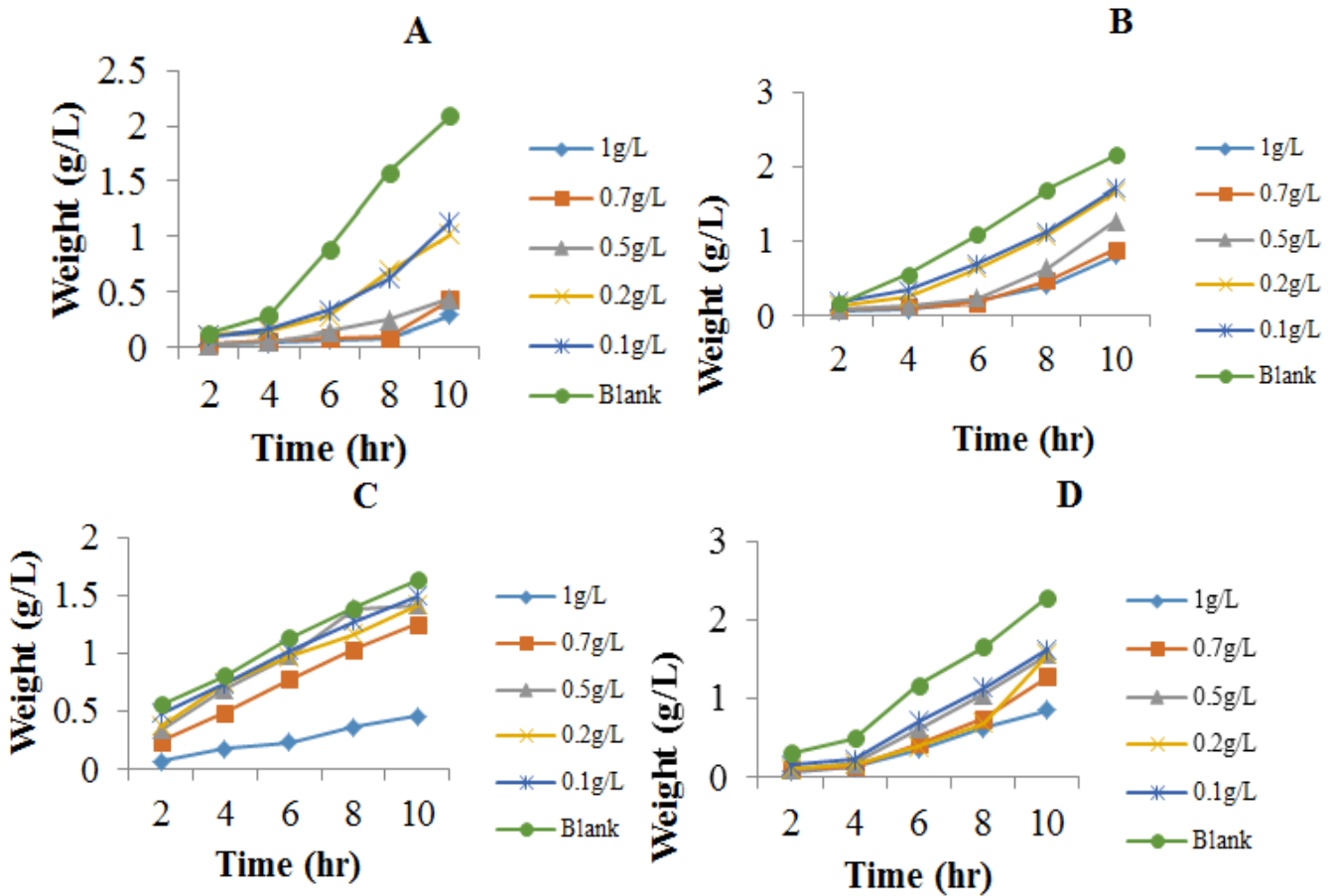
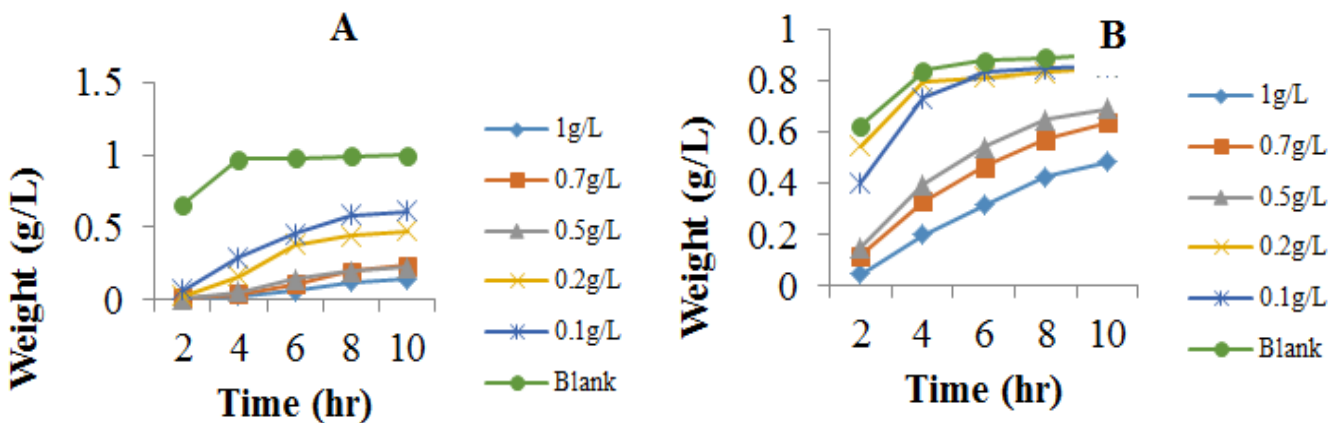


Figure 3. Variation of weight loss with time for the corrosion of mild steel in different concentrations of MLE at A (303 K), B (313 K), C (323 K) and D (333 K).



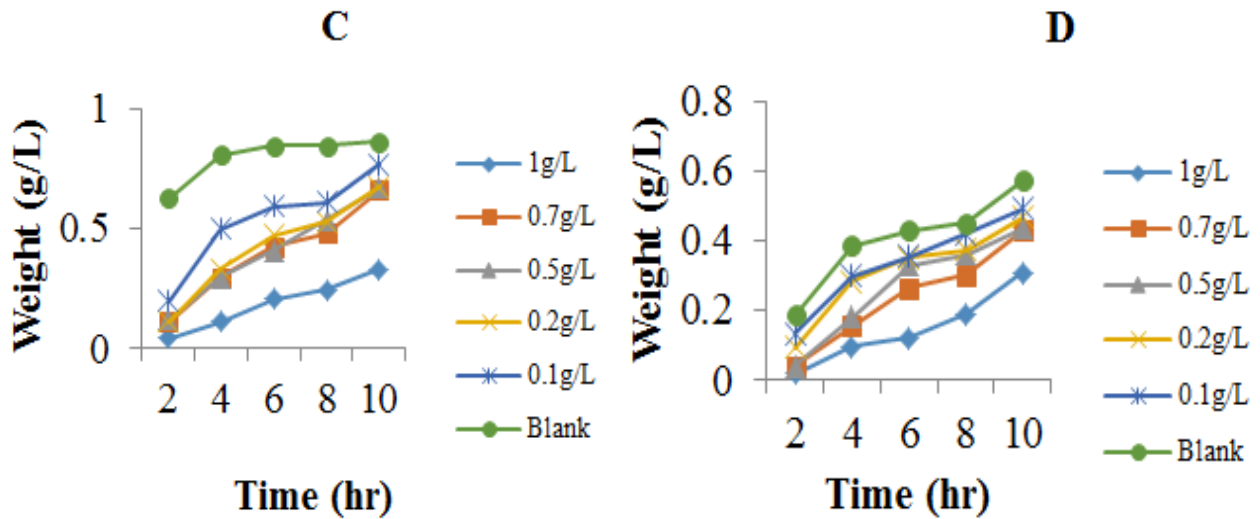


Figure 4. Variation of weight loss with time for the corrosion of aluminium in different concentrations of MSE at A (303 K), B (313 K), C (323 K) and D (333 K).

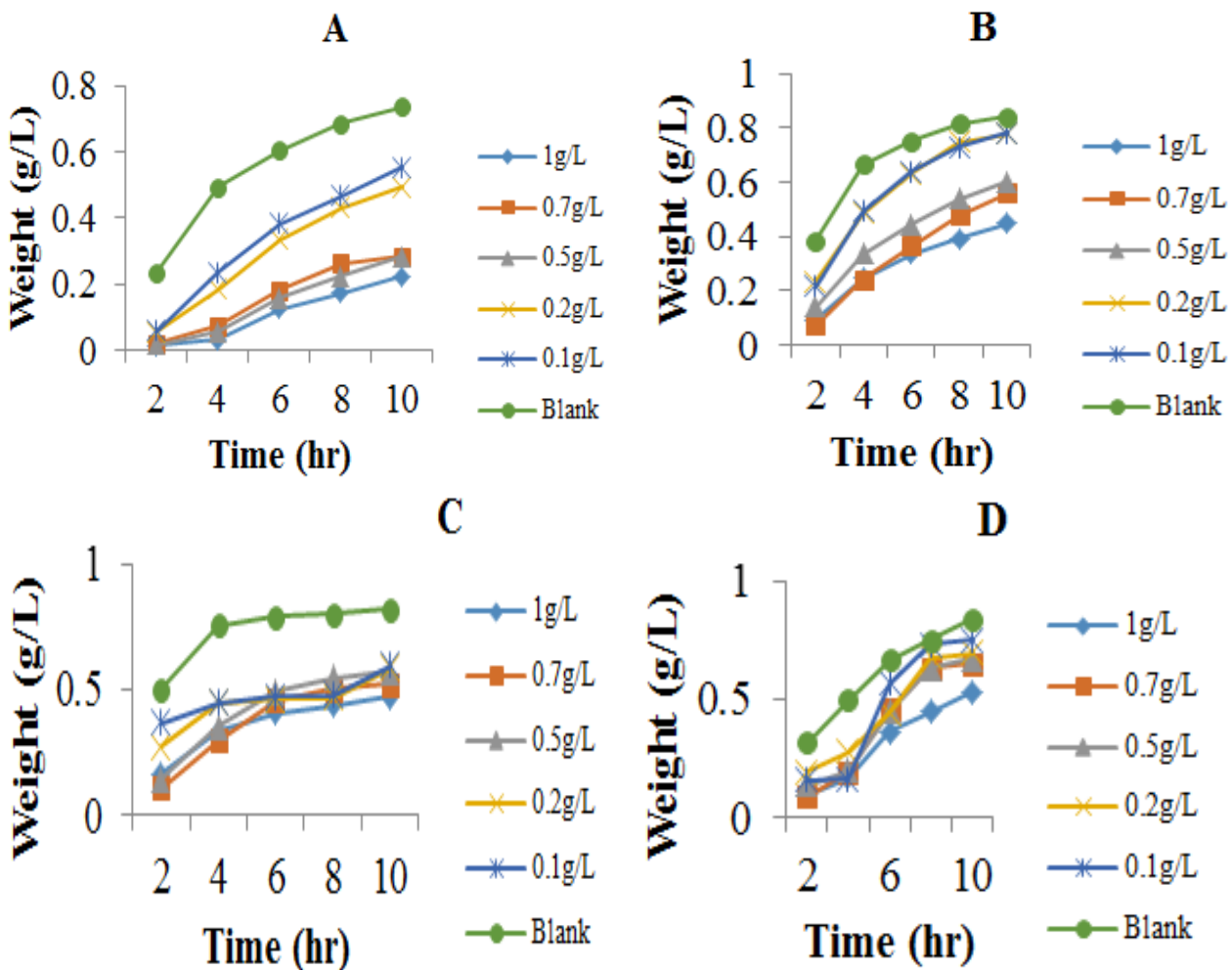


Figure 5. Variation of weight loss with time for the corrosion of aluminium in different concentrations of MLE at A (303 K), B (313 K), C (323 K) and D (333 K).

3.3 Corrosion rate and Inhibition efficiency

The corrosion rate (CR), degree of surface coverage (Θ) and inhibition efficiency (% IE) of mild steel are presented tables 3 and 4. The corrosion rate decreased with increase in concentration of all the inhibitors. Inhibition efficiency from Figures 6 and 7 increased with increase in concentration. The stem extracts (MSE) showed higher inhibition efficiency of 88% and 86% at 313 K for mild steel and 303 K for aluminium respectively with the concentration of 1 g/L. Thus, the inhibitors show significant inhibitive efficiency following the trend: MSE > MLE

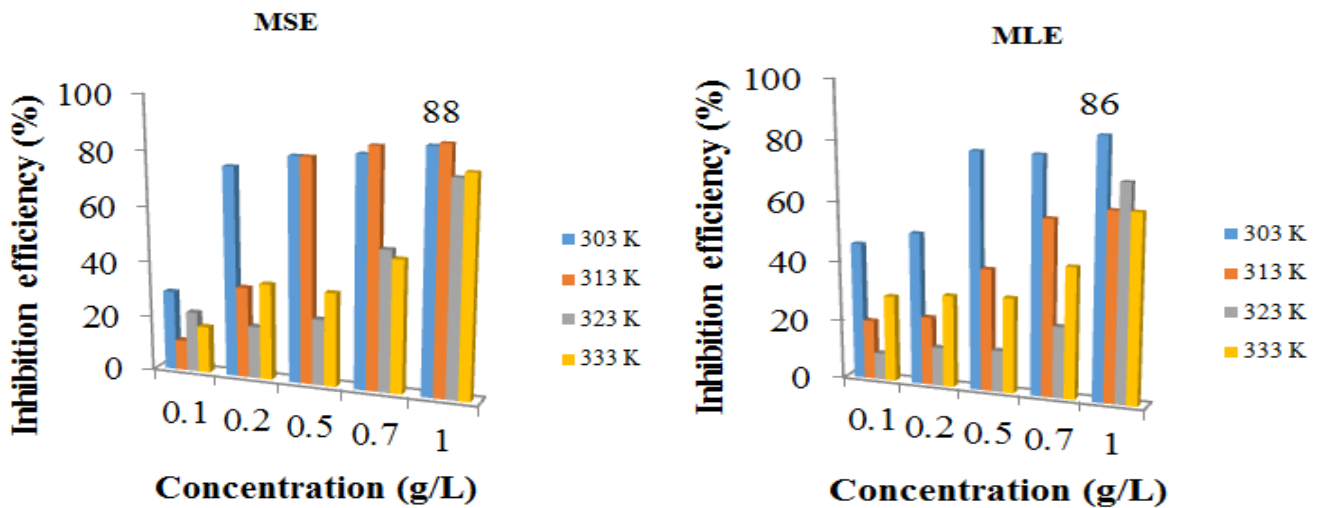


Figure 6. Variation of inhibition efficiencies of MSE and MLE with concentration and temperature for mild steel.

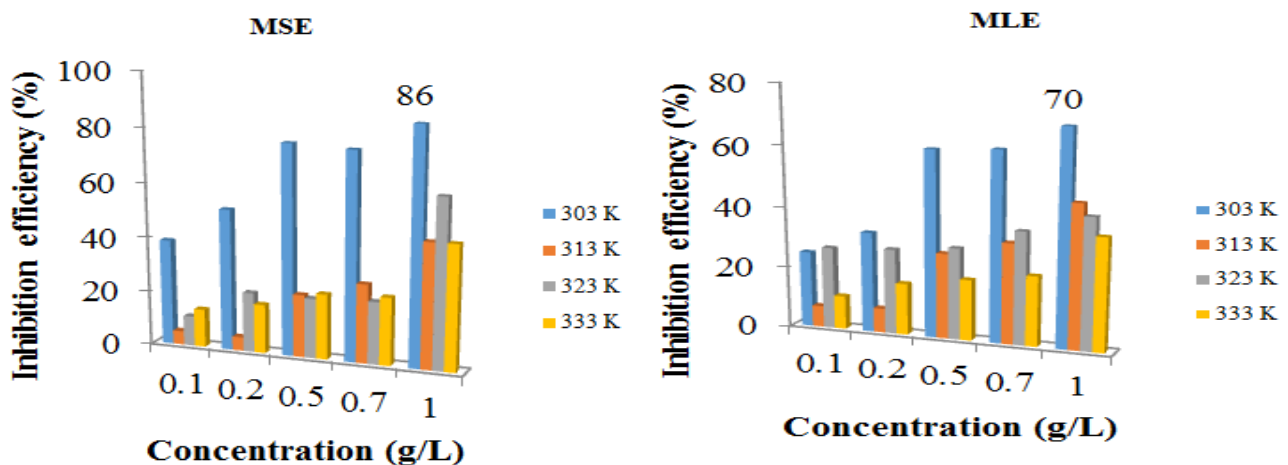


Figure 7. Variation of inhibition efficiencies of MSE and MLE with concentration and temperature for aluminium.

3.4 Activation parameters

Mild steel and aluminium corrosion is influenced by change in temperature (Saraswat *et al.*, 2020). It is described by Arrhenius equation:

$$CR = A \exp \left[\frac{-E_a}{RT} \right] \quad (2)$$

$$\log CR = \log A - \frac{E_a}{2.303RT} \quad (3)$$

Where CR is the corrosion rate of mild steel and aluminium determined from the gravimetric experiment, A is the Arrhenius or pre-exponential constant, E_a is the apparent activation energy, R is the molar gas constant ($8.314 \text{ JK}^{-1}\text{mol}^{-1}$) and T is the absolute temperature.

Table 3. Values of CR, Θ and %IE of *C. lucansianus* extracts at 303 K to 333 K for mild steel

	Conc. (g/L)	303 K			313 K			323 K			333 K		
		CR $\text{g/cm}^2\text{h} \times 10^{-3}$	Θ	% IE	CR $\text{g/cm}^2\text{h} \times 10^{-3}$	Θ	% IE	CR $\text{g/cm}^2\text{h} \times 10^{-3}$	Θ	% IE	CR $\text{g/cm}^2\text{h} \times 10^{-3}$	Θ	% IE
MSE	Blank	4.09	-	-	9.11	-	-	11.01	-	-	11.01	-	-
	0.1	2.91	0.29	29	8.13	0.11	11	8.58	0.22	22	9.18	0.17	17
	0.2	0.98	0.76	76	6.11	0.33	33	8.93	0.19	19	7.21	0.35	35
	0.5	0.76	0.81	81	1.75	0.81	81	8.33	0.24	24	7.30	0.34	34
	0.7	0.69	0.83	83	1.25	0.86	86	5.39	0.51	51	5.75	0.48	48
	1	0.55	0.87	87	1.10	0.88	88	2.48	0.77	77	2.35	0.79	79
MLE	Blank	11.63	-	-	12.00	-	-	9.09	-	-	12.68	-	-
	0.1	6.30	0.46	46	9.57	0.20	20	8.32	0.09	9	9.02	0.29	29
	0.2	5.68	0.51	51	9.29	0.23	23	7.87	0.13	13	8.71	0.31	31
	0.5	2.45	0.79	79	7.05	0.41	41	7.86	0.14	14	8.66	0.32	32
	0.7	2.42	0.79	79	4.91	0.59	59	6.95	0.24	24	7.08	0.44	44
	1	1.64	0.86	86	4.45	0.63	63	2.56	0.72	72	4.70	0.63	63

Table 4. Values of CR, Θ and %IE of *C. lucansianus* extracts at 303 K to 333 K for aluminium

	Conc. (g/L)	303 K			313 K			323 K			333 K		
		CR $\text{g/cm}^2\text{h}\times 10^{-3}$	Θ	% IE	CR $\text{g/cm}^2\text{h}\times 10^{-3}$	Θ	% IE	CR $\text{g/cm}^2\text{h}\times 10^{-3}$	Θ	% IE	CR $\text{g/cm}^2\text{h}\times 10^{-3}$	Θ	% IE
MSE	Blank	9.94	-	-	8.99	-	-	8.61	-	-	5.72	-	-
	0.1	6.10	0.39	39	8.53	0.05	5	7.68	0.11	11	4.93	0.14	14
	0.2	4.76	0.52	52	8.50	0.05	5	6.73	0.22	22	4.68	0.18	18
	0.5	2.24	0.77	77	6.88	0.23	23	6.68	0.22	22	4.37	0.24	24
	0.7	2.40	0.76	76	6.35	0.29	29	6.63	0.23	23	4.30	0.25	25
	1	1.39	0.86	86	4.84	0.46	46	3.31	0.62	62	3.08	0.46	46
MLE	Blank	7.38	-	-	8.41	-	-	8.18	-	-	8.42	-	-
	0.1	5.55	0.25	25	7.84	0.07	7	5.98	0.27	27	7.53	0.11	11
	0.2	4.95	0.33	33	7.77	0.08	8	5.88	0.28	28	6.97	0.17	17
	0.5	2.84	0.61	61	6.03	0.28	28	5.70	0.30	30	6.70	0.20	20
	0.7	2.84	0.62	62	5.62	0.33	33	5.19	0.37	37	6.52	0.23	23
	1	2.24	0.70	70	4.48	0.47	47	4.70	0.43	43	5.34	0.37	37

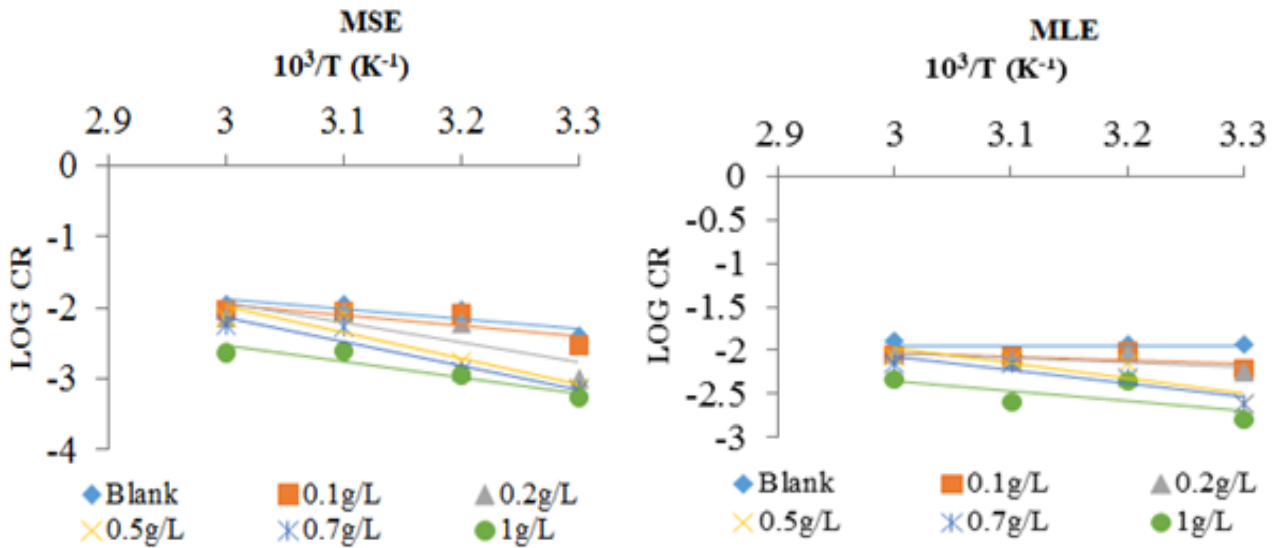


Figure 8. Arrhenius plot (log CR versus $10^3/T$) for aluminium in different concentrations of MSE and MLE.

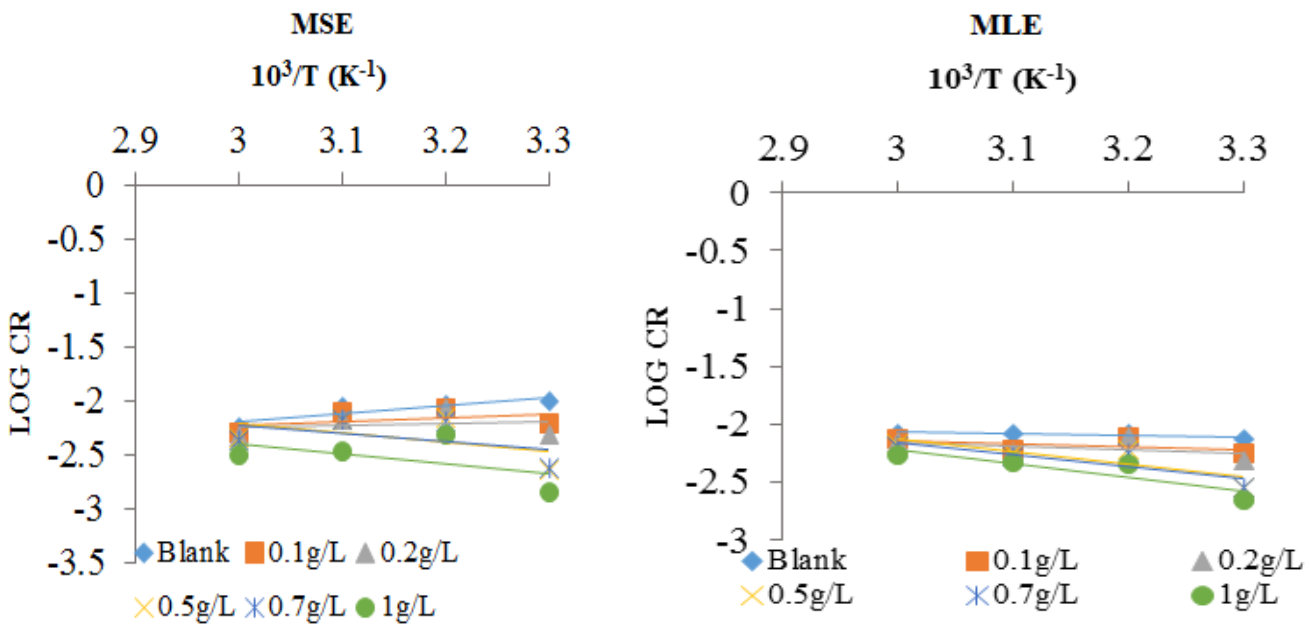


Figure 9. Arrhenius plot (log CR versus $10^3/T$) for aluminium in different concentrations of MSE and MLE.

The values of activation energies graphically presented in Tables 5 and 6 explicitly explain that the presence of the inhibitors increased the activation energy (E_a) of the reaction indicating an adsorption process and implying that the adsorption of stem and leave extract of *C. lucanusianus* (MSE and MLE) on mild steel and aluminium surfaces is responsible for the formation of the barrier layer that retards the metal activity in the electrochemical reactions of corrosion (Obot, 2011).

Table 5. Activation parameters from Arrhenius equation for mild steel in different concentrations of MSE and MLE at 303 K to 333 K

Inhibitor	Conc. (g/L)	ACTIVATION PARAMETERS				
		Intercept	Slope	E_a (J/mol)	A ($\text{gcm}^{-2}\text{h}^{-1}$)	R^2
MSE	Blank	2.2412	-1.3738	11.42	9.40	0.7468
	0.1	2.6038	-1.5194	12.63	13.52	0.6873
	0.2	6.3777	-2.7719	23.05	588.58	0.6523
	0.5	8.9091	-3.6294	30.18	7398.98	0.8690
	0.7	8.0627	-3.3988	28.26	3173.84	0.9038
	1	4.2203	-2.2488	18.70	68.05	0.8763
MLE	Blank	-1.9755	0.0086	-0.07	0.14	0.0003
	0.1	-0.8023	-0.4076	3.39	0.45	0.4272
	0.2	-0.5845	-0.4844	4.03	0.56	0.4351
	0.5	3.0965	-1.6917	14.07	22.12	0.7343
	0.7	2.5791	-1.5517	12.90	13.19	0.8430
	1	1.0642	-1.1360	9.45	2.90	0.4560

Table 6. Activation parameters from Arrhenius equation for aluminium in different concentrations of MSE and MLE at 303 K to 333 K.

Inhibitor	Conc. (g/L)	ACTIVATION PARAMETERS				
		Intercept	Slope	E_a (J/mol)	A ($\text{gcm}^{-2}\text{h}^{-1}$)	R^2
MSE	Blank	-4.4175	0.7391	-6.15	0.01	0.8148
	0.1	-3.1919	0.3224	-2.68	0.04	0.1534
	0.2	-2.6173	0.1249	-1.04	0.07	0.0165
	0.5	0.3562	-0.8549	7.11	1.43	0.2363
	0.7	0.1141	-0.7793	6.48	1.12	0.2415
	1	0.2104	-0.8736	7.26	1.23	0.2448
MLE	Blank	-1.5901	-0.1594	1.33	0.20	0.5754
	0.1	-1.2972	-0.2793	2.32	0.27	0.2400
	0.2	-1.1760	-0.3253	2.70	0.31	0.2387
	0.5	1.1489	-1.0937	9.09	3.15	0.6941
	0.7	0.9899	-1.0498	8.73	2.69	0.7277
	1	1.2411	-1.1558	9.61	3.46	0.7672

3.5 Thermodynamic Parameters

The transition state equation was used to calculate the enthalpy change (ΔH) and the entropy change (ΔS) for the formation of the activation complex (Ameh *et al.*, 2015; Ituen and Udo, 2012).

$$CR = \frac{RT}{N_h} \exp\left(\frac{\Delta S}{R}\right) \exp\left(\frac{-\Delta H}{RT}\right) \quad (4)$$

$$\log \frac{CR}{T} = \log\left(\frac{R}{N_h}\right) + \left(\frac{\Delta S}{2.303R}\right) - \left(\frac{\Delta H}{2.303RT}\right) \quad (5)$$

Where CR is the corrosion rate of mild steel and aluminium determined from the gravimetric experiment, R is the universal gas constant ($8.314 \text{ JK}^{-1}\text{mol}^{-1}$), N is the Avogadro's number ($6.02214 \times 10^{23} \text{ mol}^{-1}$), h is Planck's constant ($6.62607 \times 10^{-34} \text{ Js}$), T is the absolute temperature, ΔH is enthalpy change and ΔS is entropy change.

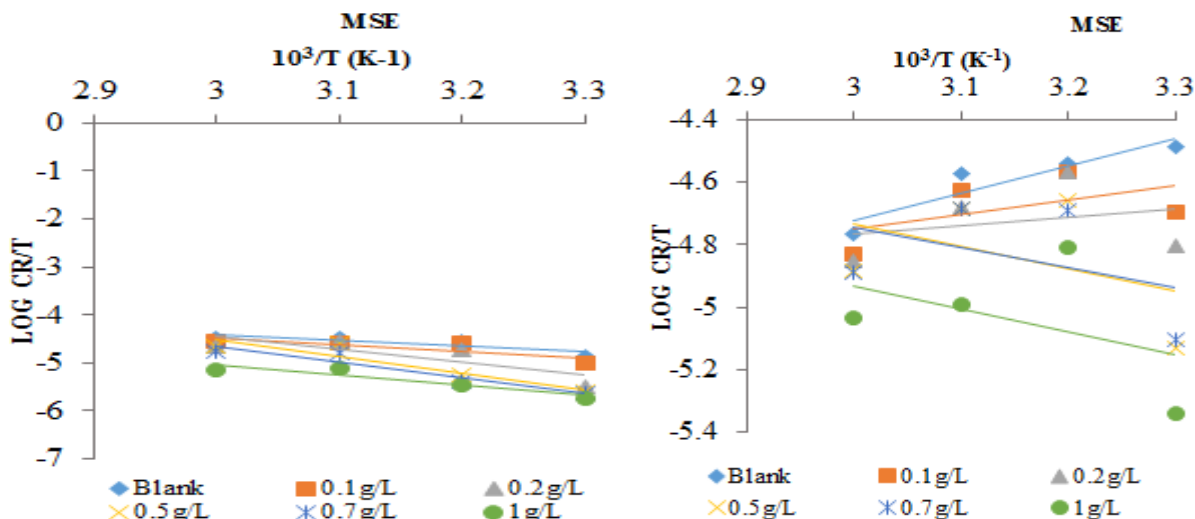


Figure 10. Transition state plot ($\log CR/T$ versus $10^3/T$) for mild steel in different concentrations of MSE and MLE.

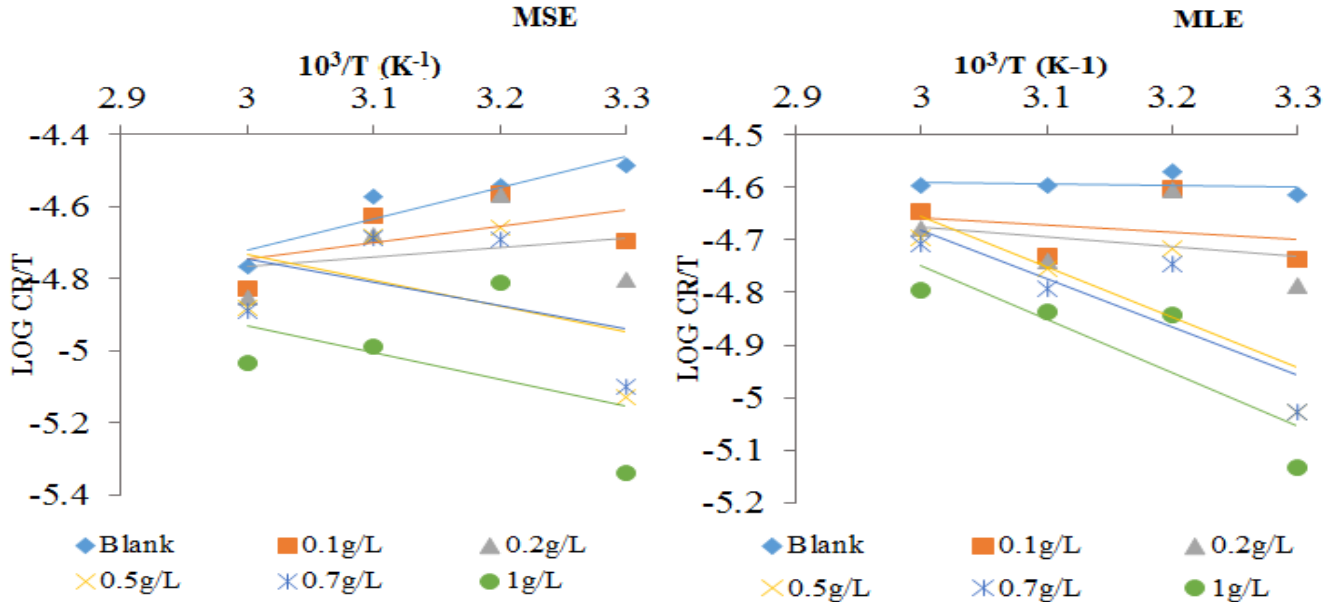


Figure 11. Transition state plot (log CR/T versus $10^3/T$) for aluminium in different concentrations of MSE and MLE.
Table 7. Activation parameters from Transition State equation for mild steel in different concentrations of MSE and MLE at 303 K to 333 K.

Inhibitor	Conc. (g/L)	ACTIVATION PARAMETERS				
		Intercept	Slope	ΔH (J/mol)	ΔS (J/mol.K)	R^2
MSE	Blank	-0.6915	-1.2371	23.6877	-210.8156	0.7062
	0.1	-0.3288	-1.3827	26.4754	-203.8715	0.6462
	0.2	3.4451	-2.6353	50.4581	-131.6122	0.6295
	0.5	5.9764	-3.4928	66.8766	-83.1436	0.8602
	0.7	5.1300	-3.2622	62.4614	-99.3497	0.8965
	1	1.2877	-2.1121	40.4411	-172.9206	0.8625
MLE	Blank	-4.9081	0.1453	-2.7814	-291.5521	0.0791
	0.1	-3.7349	-0.2709	5.1870	-269.0887	0.2489
	0.2	-3.5171	-0.3478	6.6589	-264.9187	0.2852
	0.5	0.1639	-1.5551	29.7753	-194.4377	0.7010
	0.7	-0.3535	-1.4150	27.0933	-204.3440	0.8179
	1	-1.8685	-0.9994	19.1353	-233.3518	0.3937

Table 8. Activation parameters from Transition State equation for aluminium in different concentrations of MSE and MLE at 303 K to 333 K.

Inhibitor	Conc. (g/L)	ACTIVATION PARAMETERS				
		Intercept	Slope	ΔH (J/mol)	ΔS (J/mol.K)	R^2
MSE	Blank	-7.3502	0.8758	-16.7690	-338.3102	0.8618
	0.1	-6.1246	0.4590	-8.7889	-314.8435	0.2697
	0.2	-5.5499	0.2616	-5.0086	-303.8406	0.0689
	0.5	-2.5765	-0.7182	13.7515	-246.9077	0.1796
	0.7	-2.8186	-0.6427	12.3056	-251.5436	0.1784
	1	-2.7223	-0.7369	14.1094	-249.6994	0.1878
MLE	Blank	-4.5228	-0.0228	0.4359	-284.1739	0.0274
	0.1	-4.2298	-0.1426	2.7309	-278.5641	0.0762
	0.2	-4.1087	-0.1886	3.6117	-276.2445	0.0957
	0.5	-1.7837	-0.9570	18.3240	-231.7284	0.6356
	0.7	-1.9427	-0.9131	17.4835	-234.7732	0.6700
	1	-1.6915	-1.0192	19.5143	-229.9630	0.7203

The positive values of ΔH indicate that the adsorption process is endothermic. The negative values of ΔS indicate a decrease in the disorderliness of the system and therefore an increased orderliness in the system as a result of an orderly adsorption of the inhibitor molecules freely moving in the bulk solution onto the mild steel and aluminium metal surfaces

3.6 Adsorption Parameters

Langmuir, Temkin, Freundlich and El-Awady were investigated. All these isotherms can be represented as follows:

$$f(\theta, x) \exp(-2a\theta) = K_{ads}C \quad (6)$$

where $f(\theta, x)$ represents the configuration factor dependent on the physical model and assumptions underlying the derivation of the particular model, a is the molecular interaction parameter used to predict the nature of interactions in the adsorbed layer, K_{ads} is the adsorption equilibrium constant which describes how strongly the molecules are held on the adsorbent surface and C is the inhibitor concentration (Ituen *et al.*, 2017). Freundlich adsorption isotherm was perfectly obeyed (figure 12 and 13) and it Freundlich adsorption isotherm described the adsorptive behaviour of the extracts of *C. lucanusianus* presented in Tables 9 and 10.

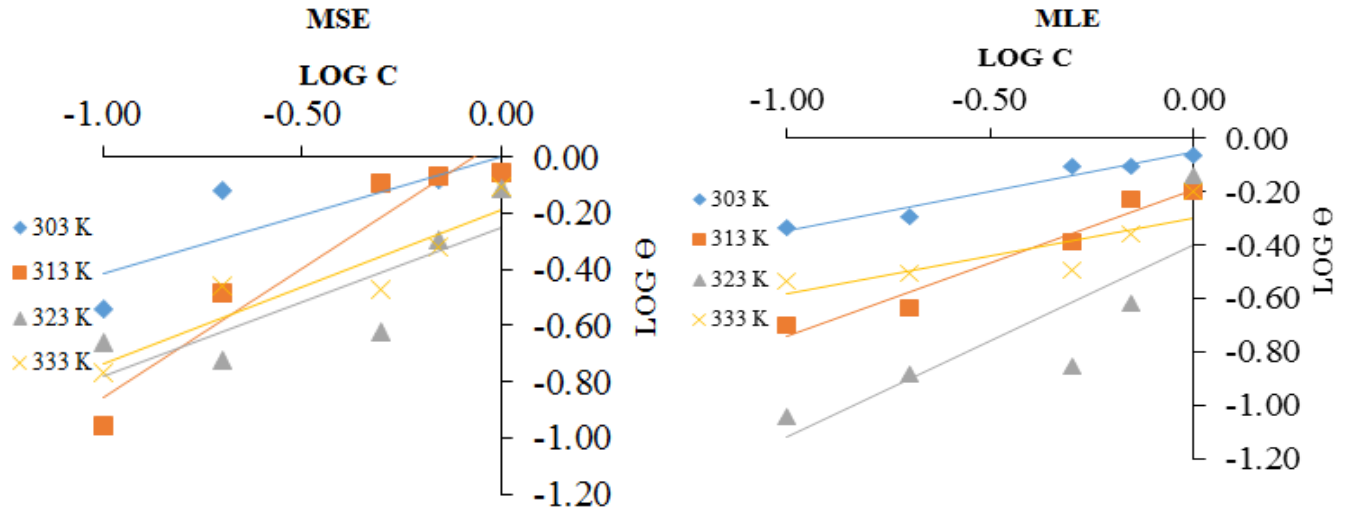


Figure 12. Freundlich adsorption isotherm plot (C/Θ versus C) for mild steel in different concentrations of MSE and MLE.

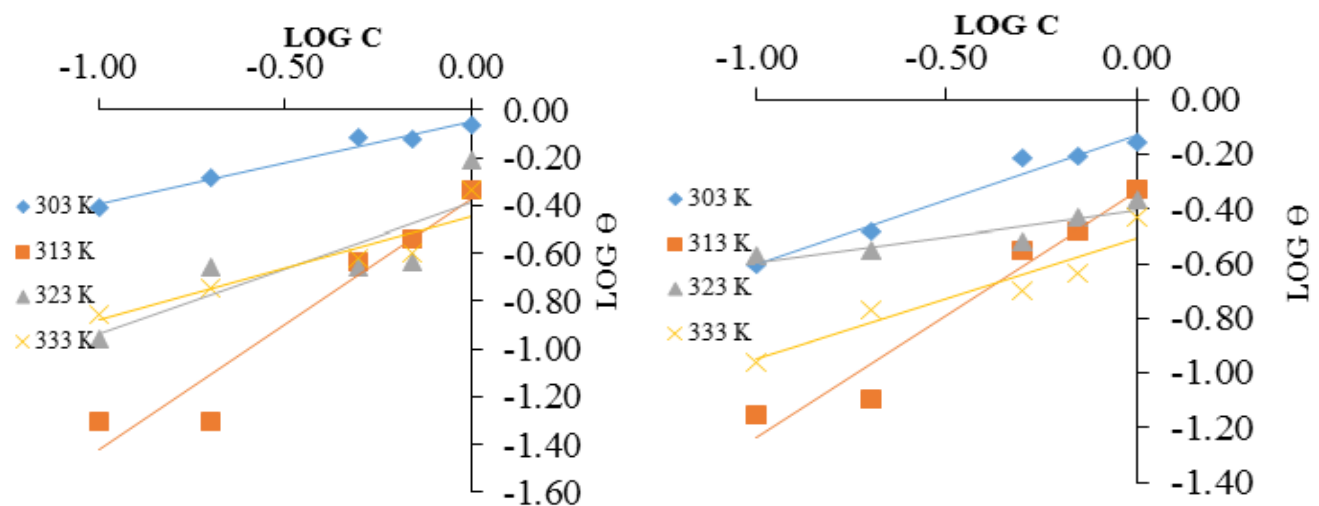


Figure 13. Freundlich adsorption isotherm plot (C/Θ versus C) for aluminium in different concentrations of MSE and MLE.

Negative values of ΔG_{ads} (Tables 9 and 10) show that the inhibitor molecules are spontaneously adsorbed on the metal surface (Ituen *et al.*, 2017). The mechanism of adsorption is physisorption since the value of $\Delta G_{ads} \leq -20 \text{ kJmol}^{-1}$ (El-Awady *et al.*, 2008; Oguzie, 2007; El-Sherif and Badawy, 2011).

Table 9. Adsorption parameters from Freundlich isotherm for mild steel in different concentrations of MSE and MLE at 303 K to 333 K.

Inhibitor	Temp (K)	ADSORPTION PARAMETERS					
		Intercept	Slope / n	1/n	K_{ads} (mol/l)	ΔG (kJ/mol)	R^2
MSE	303 K	-0.0006	0.4115	2.4300	0.9994	-4.3915	0.6986
	313 K	0.0660	0.9201	1.0868	1.0683	-4.8490	0.9206
	323 K	-0.2526	0.5297	1.8878	0.7768	-3.6385	0.6789
	333 K	-0.1885	0.5442	1.8374	0.8282	-3.9997	0.8432
MLE	303 K	-0.0519	0.2972	3.3644	0.9494	-4.1720	0.9530
	313 K	-0.1952	0.5467	1.8292	0.8226	-3.7341	0.9576
	323 K	-0.3972	0.7250	1.3794	0.6722	-3.1487	0.7169
	333 K	-0.2963	0.2862	3.4947	0.7435	-3.5907	0.6953

Table 10. Adsorption parameters from Freundlich isotherm for aluminium in different concentrations of MSE and MLE at 303 K to 333 K.

Inhibitor	Temp (K)	ADSORPTION PARAMETERS					
		Intercept	Slope / n	1/n	K_{ads} (mol/l)	ΔG (kJ/mol)	R^2
MSE	303 K	-0.0494	0.3453	2.8957	0.9518	-4.1824	0.9715
	313 K	-0.3679	1.0561	0.9469	0.6922	-3.1420	0.9303
	323 K	-0.3871	0.5494	1.8201	0.6790	-3.1805	0.7074
	333 K	-0.4441	0.4349	2.2992	0.6414	-3.0975	0.8514
MLE	303 K	-0.1279	0.4739	2.1100	0.8800	-3.8666	0.9718
	313 K	-0.3362	0.8971	1.1147	0.7145	-3.2432	0.9527
	323 K	-0.4076	0.1877	5.3277	0.6652	-3.1160	0.7964
	333 K	-0.5087	0.4427	2.2590	0.6013	-2.9038	0.8963

Table 11. Optimized structure, HOMO and LUMO orbital distribution of the major compounds contained in *C. lucanusianus*.

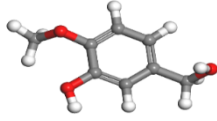
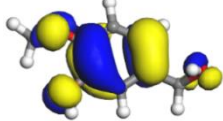
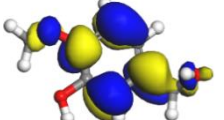
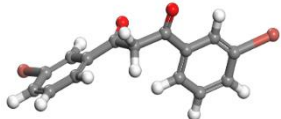
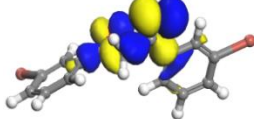
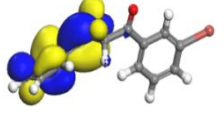
	Molecular Formula	Compound	Optimized Structure	HOMO orbital distribution	LUMO orbital distribution
MSE	C ₈ H ₁₀ O ₃	3-hydroxy-4-methoxy benzylalcohol			
MLE	C ₁₅ H ₁₀ Br ₂ O ₂	1,3-bis(3-bromophenyl) propane-1,3-dione			

Table 12. Quantum reactivity parameters for MSE and MLE inhibitors.

	COMPOUNDS	HOMO (eV)	LUMO (eV)	ΔE_{gap} (eV)	IE	EA	χ	μ	η	σ	ω	ε	ΔN
MSE	1,3-bis(3-bromophenyl)propane-1,3-dione	-5.91	-3.05	2.86	5.91	3.05	4.48	-4.48	1.43	0.70	7.01	0.14	0.12
MLE	3-hydroxy-4-methoxy benzylalcohol	-5.15	-1.02	4.13	5.15	1.02	3.09	-3.09	2.06	0.49	2.31	0.43	0.42

3.7 Quantum Chemical Parameters

The compounds that are likely to be involved in the inhibition of the corrosion of mild steel and aluminium by MSE and MLE are the ones distributed all around each molecule most dominated by bonded heteroatoms (Oxygen and Nitrogen atoms) and some of the carbon atoms basically those containing unsaturated bonds in their molecule, and on the entire aromatic rings (Table 11)

The calculated electronic properties, EHOMO (electron donating ability) and ELUMO (electron accepting ability) provided information about the reactive behaviour of the molecules of the selected compounds of *C. lucanusianus* (Table 12).

Molecules are effective as corrosion inhibitor, when they donate electrons to the vacant d-orbital of the metal for bonding, and also receive free electrons from the metal surface (Ozoemena et al., 2019). Reactivity ability of an inhibitor molecule is considered closely related to their frontier molecular orbitals, such that frontier orbital theory (HOMO and LUMO orbital), was used to predict adsorption centres of the *C. lucanusianus* molecules responsible for the interaction with mild steel and aluminium metal surfaces. The HOMO orbital in an organic molecule corresponds to the electron providing capacity of a molecule and the LUMO orbital corresponds to the electron gaining capacity of a molecule (Guo et al., 2020). Generally, the higher the value of EHOMO, the greater the tendency of the inhibitor to donate electrons, and the lower the value of ELUMO, the greater the tendency of the inhibitor to accept electrons. From Table 12, values of EHOMO increased in the order n- MSE < MLE, suggesting that MLE adsorbed better on the metal surface than MSE. Accordingly, the values of ELUMO decreased in the order MLE > MSE, suggesting that MSE *C. lucanusianus* extract is a good corrosion inhibitor capable of accepting electrons from mild steel and aluminium surfaces by forming the inhibition barrier (Ozoemena et al., 2019). This confirms that the presence of the selected identified component molecules in the leave and stem extracts increased the inhibition efficiency which correlates with the experimental results (Gece, 2008).

Energy gap is the function of reactivity of the inhibition molecules toward adsorption on metallic surfaces. The smaller the value of energy gap, the greater the activity of corrosion inhibitor molecules; and the easier it is to adsorb to the metal surface, thereby showing better corrosion inhibition

performance (Guo et al., 2020). Low values of the energy gap (ΔE) provide good inhibition efficiency because the excitation energy from the last occupied orbital will be low (Gece, 2008). Calculations from Table 12 show the decreasing energy gap trend for the compounds of *C. lucanusianus* extracts in the order: MLE > MSE, suggesting that *C. lucanusianus* stem extracts provide good inhibition efficiency and this is the same order of inhibition efficiency obtained for the inhibitor experimentally.

Adsorption of inhibitor to the metal surface occurs at the part of the molecule with the greatest softness and lowest hardness (Wang, 2012). Global hardness (η) and softness (σ) are significantly related to the energy gap measuring the stability and reactivity of a molecule. Soft molecules have small energy gaps and hard molecules have large energy gap (Obi-Egbedi et al., 2011). Conversely, soft molecules with small energy gaps are efficient corrosion inhibitors since they can easily donate electrons to metal atoms at the surface (Ozoemena et al., 2019). Table 12 shows that components of *C. lucanusianus* extracts have lower values of softness (σ) and greater values of hardness (η). The softness (σ) values of the extract increase in the order: MLE < MSE and the hardness values decrease in the reverse order: MLE > MSE showing that the inhibitor with the least values of global hardness and highest values of global softness is the best. Therefore, the MSE is the more efficient and reactive than MLE and this is consistent with the results obtained from the experimental inhibition efficiencies.

The dipole moment (μ) is another index often used for prediction of relative ability of corrosion inhibitors (Bashir et al., 2020). This was calculated using ionization potential and electron affinity. It is a measure of polarity in a bond. Inhibitors with high dipole moments tend to form strong dipole-dipole interactions with the metal, which results in strong adsorption onto the metal surface, leading to greater inhibition efficiency (Sasikumar et al., 2015). The values of dipole moment indicate the possibility of adsorption of the molecules by electron donation to the unfilled orbital of iron (BoEKOM et al., 2020). The results reported in Table 12 show that MLE and n-HLE has higher dipole moments value which facilitate its adsorption to the metal surface.

Electronegative values of MSE and MLE are given as 4.48 and 3.09 respectively. These values are lower than the work function of Fe (110) surface given as 4.82 indicating electron migration from the inhibitor to the Fe surface (Abakedi et al., 2020).

Electron transfer direction and intensity are demonstrated by ΔN values (Saraswat *et al.*, 2020). The values of ΔN shown in Table 12 are positive suggesting that the transfer of electron was from the inhibitor to vacant orbital of the metal. Since the ΔN values are lower than 3.6, the inhibition efficiency increase with increasing electron donating ability of the inhibitor on the metal surface according to Lukovits's studies (Lukovits *et al.*, 2001; Emregül and Hayvalı, 2006).

Conclusion

The inhibitor, *C. lucanusianus* (MSE and MLE) showed significant inhibitive effects at all concentrations; the stem extracts (MSE) showed higher inhibition efficiency of 88% and 86% for both mild steel and aluminium; at 313 K for mild steel and 303 K for aluminium respectively at the concentration of 1 g/L. The adsorption of active components of inhibitor obeys Freundlich adsorption isotherm. Experimental inhibition efficiencies of these inhibitors were found to be closely related to the quantum chemical parameters. The inhibitors showed significant inhibitive effect following the trend: MSE > MLE for mild steel and aluminium. This trend suggests that these inhibitors act through adsorption on mild steel and aluminium surfaces; and the formation of a barrier layer between the metal and the corrosive medium.

References

Abakedi, O.U., Mkpenie, V.N. and Ukpong, E G. (2020). Anti-corrosion behaviour of 4(p-tolyldiazonyl)-2-((E)-(p-tolylimino)methyl) phenol on mild steel in 1M H₂SO₄: Experimental and theoretical studies. *Scientific African*, 7: 1–14.

Ameh, P.O., Koha, P.U. and Eddy, N.O. (2015). Experimental and quantum chemical studies on the corrosion inhibition potential of phthalic acid for mild steel in 0.1 M H₂SO₄. *Chemical Sciences Journal*, 6(3): 1–8.

Aralu, C.C., Chukwuemeka, H.O. and Kovo, O. (2021). Inhibition and adsorption potentials of mild steel corrosion using methanol extract of *Gongronema latifolium*. *Applied Water Science*, 11(2), 1–7.

Bashir, S., Sharma, V., Ghelichkhah, Z., Obot, I. B. and Kumar, S. (2020). Inhibition performances of nicotinamide against aluminium corrosion in an acidic medium. *Portugaliae Electrochimica Acta*, 38(2): 107–123.

Belghiti, M. E., Echihi, S., Dafali, A., Karzazi, Y., Bakasse, M. and Elalaoui-elabdallaoui, H. (2019). Computational simulation and statistical analysis on the relationship between corrosion inhibition efficiency and molecular structure of some hydrazine derivatives in phosphoric acid on mild steel surface. *Applied Surface Science*, 491: 707–722.

BoEKOM, E., Essien, K. E., Ekpo, V. F. and Obot, A. (2020). Kinetics, molecular dynamics and adsorption behaviour of pyridine on mild steel in 0.1M HCl solution. *Elixir Applied Chemistry*, 142: 54382–54387.

Lukovits, I., Kalman, E. and Zucchi, F. (2001). Corrosion inhibitors: Correlation between electronic structure and efficiency. *Corrosion Science*, 57(1): 3–8.

Mahgoub, F. M., Hefnawy, A. M. and Alrazzaq, E. H. A. (2019). Corrosion inhibition of mild steel in acidic solution by leaves and stem extract of *Acacia nilotica*. *Desalination and Water Treatment*, 169: 49–58.

Obi-Egbedi, N. O., Obot, I. B., El-Khajary, M. I., Umoren, S. A. and Ebenso, E. E. (2011). Computational simulation and statistical analysis on the relationship between corrosion inhibition efficiency and molecular structure of some phenanthroline derivatives on mild steel surface.

El-Awady, G. Y., El-Said, I. A. and Fouda, A. S. (2008). Anion surfactants as corrosion inhibitors for aluminium dissolution in HCl solutions. *International Journal of Electrochemical Science*, 3: 174–190.

El-Etre, A. Y. (2008). Inhibition of C-steel corrosion in acidic solution using the aqueous extract of *Zallouh* root. *Materials Chemistry and Physics*, 108: 278–282.

El-Sherif, R. M. and Badawy, W. A. (2011). Mechanism of corrosion and corrosion inhibition of tin in aqueous solution containing tartaric acid. *International Journal of Electrochemical Science*, 6: 6469–6482.

Emregül, K. C. and Hayvalı, M. (2006). Studies on the effect of a newly synthesized Schiff base compound from phenazone and vanillin on the corrosion of steel in 2 M HCl. *Corrosion Science*, 48: 797–812.

Gece, G. (2008). The use of quantum chemical methods in corrosion inhibitor studies. *Corrosion Science*, 50(11): 2981–2992.

Geetha, K. and Udhayakumar, R. (2021). A green tactic for inhibition of corrosion on mild steel in bore well water by aqueous extract of *Bauhinia Blakeana* leaves. *Indian Journal of Chemical Technology*, 28: 36–46.

Guo, L., Tan, B., Li, W., Li, Q., Zheng, X. and Bassey, I. (2020). Banana leaves water extracts as inhibitor for X70 steel corrosion in HCl medium. *Journal of Molecular Liquids*, 327: 114828–114839.

Hsissou, R., Benhiba, F., Dagdag, O., El-Bouchti, M., Nouneh, K., Assouag, M. and Elharfi, A. (2020). Development and potential performance of pre-polymer in corrosion inhibition for carbon steel in 1.0 M HCl: Outlooks from experimental and computational investigations. *Journal of Colloid and Interface Science*, 574: 43–60.

Ituen, E. I. and Udo, U. E. (2012). Phytochemical profile, adsorption and inhibitive behaviour of *costus afer* extracts on aluminium corrosion in hydrochloric acid. *Pelagia Research Library*, 3(6): 1394–1405.

Ituen, E., Akaranta, O. and James, A. (2017). Evaluation of performance of corrosion inhibitors using adsorption isotherm models: An overview. *Chemical Science International Journal*, 18(1): 1–34.

Ituen, E., Mkpenie, V., Moses, E. and Obot, I. (2019). Electrochemical kinetics, molecular dynamics, adsorption and anticorrosion behavior of melatonin biomolecule on steel surface in acidic medium. *Bioelectrochemistry*, 129: 42–53

Lakmal, O. H. and Tillekaratne, A. (2018). Optimization and characterization of a green corrosion inhibitor using *Costus speciosus* extract for the corrosion of mild steel in 1 M HCl. *Research Journal of Chemical Sciences*, 8(1): 18–22.

Lopez, B., Valdez, B., Zlatev, R., Flores, J., Carrillo, M. and Schorr, M. (2007). Corrosion of metals at indoor conditions in the electronics manufacturing industry. *Anti-Corrosion Methods and Materials*, 54(6): 354–359.

International Journal of Electrochemical Science, 6, 5649–5675.

Obot, I. B. (2011). Chemical investigation of xanthene and phenanthroline derivatives as corrosion inhibitors for mild steel in sulphuric acid. Ph.D Thesis. University of Ibadan.

Oguzie, E. E., Akalezi, C. O., Okoro, S. C., Ayuk, A. A. and Ejike, E. N. (2010). Adsorption and corrosion inhibiting effect of *Dacryodis edulis* extracts on low-carbon-steel corrosion in acidic medium. *Journal of Colloid and Interface Science*, 349(1): 283–292.

Olasunkanmi, L. and Ebenso, E. (2020). Experimental and computational studies on propanone derivatives of

quinoxalin-6-yl-4,5-dihydropyrazole as inhibitors of mild steel corrosion in hydrochloric acid. *Journal of Colloid and Interface Science*, 561: 104–116.

Othman, N., Yahya, S. and Ismail, M. (2019). Corrosion inhibition of steel in 3.5% NaCl by rice straw extract. *Journal of Industrial Engineering and Chemistry*, 70: 299–310.

Ozoemena, C. P., Charles, M., Ugwuoke, M. C. and Akpan, G. (2019). Adsorption and quantum chemical studies on the inhibition potentials of *Azela africana* seed extract for the corrosion of mild steel in 2 M HCl solutions. *International Journal of Research and Innovation in Applied Science*, 4(11): 24–32.

Saraswat, V., Yadav, M. and Obot, I. B. (2020). Investigations on eco-friendly corrosion inhibitors for mild steel in acid environment: Electrochemical, DFT and Monte Carlo simulation approach. *Colloids and Surfaces A: Physicochemical and Engineering Aspects*, 599(4): 124881–124899

Saratha, R. and Meenakshi, R. (2010). Corrosion inhibitor: A plant extract. *Der Pharma. Chemica*, 2(1): 287–294.

Sasikumar, Y., Adekunle, A., Olasunkanmi, L., Bahadur, I., Baskar, R., Kabanda, M. and Ebenso, E. (2015). Experimental, quantum chemical and monte carlo simulation studies on the corrosion inhibition of some alkyl imidazolium ionic liquids containing tetrafluoroborate anion on mild steel in acidic medium. *Journal of Molecular Liquids*, 211: 105–118.

Segneanu, A., Sfirloaga, P., Balci, I., Vlatanescu, N. and Grozescu, I. (2012). A comparative study between different corrosion protection layers, pp139–154 In: B. Valdez, and M. Schorr, (Ed.). *Environmental and Industrial Corrosion - Practical and Theoretical Aspects*. Intechopen Books, London, United Kingdom.

Tan, B., He, J., Zhang, S., Xu, C., Chen, S., Liu, H. and Li, W. (2020). Insight into anti-corrosion nature of *Betel* leaves water extracts as the novel and eco-friendly inhibitors. *Journal of Colloid and Interface Science*, 585: 287–301.

Uwah, I., Ikeuba, A., Ugi, B. and Udowo, V. (2013a). Comparative study of the inhibition effects of alkaloid and non-alkaloid fractions of the ethanolic extracts of *Costus afer* stem on the corrosion of mild steel in 5 M HCl solution. *Global Journal of Pure and Applied Sciences*, 19(1): 23–31.

Uwah, I. E., Ugi, B. U., Ikeuba, A. I. and Etuk, K. E. (2013b). Evaluation of the inhibitive action of eco-friendly benign *Costus afer* stem extract on the corrosion of mild steel in 5 M HCl solution. *International Journal of Development and Sustainability*, 2(4): 1970–1981.

Valdez, B., Zlatev, R., Schorr, M., Rosas, N., Dobrev, T., Monev, M., and Krastev, I. (2006). Rapid method for corrosion protection determination of VCI films. *Anti-Corrosion Methods and Materials*, 53(6): 362–366.

Wang, Z. (2012). The inhibition effect of bis-benzimidazole compound for mild steel in 0.5 M HCl solution. *International Journal of Electrochemical Science*, 7: 11149–11160.